MAX-PLANCK-INSTITUT FÜR PLASMAPHYSIK

GARCHING BEI MÜNCHEN

High-Efficiency Toroidal Current Drive Using Low-Phase-Velocity Kinetic Alfvén Waves

Satish Puri

IPP 4/248 September 1991

IAEA Technical Committee Meeting
on Fast Wave Current Drive in Reactor Scale Tokamaks
Latitudes CAMARGUE, ARLES (FRANCE)
September 23 – 25, 1991, (to be published)

HIGH-EFFICIENCY TOROIDAL CURRENT DRIVE USING LOW-PHASE-VELOCITY KINETIC ALFVÉN WAVES

S. PURI
Max-Planck-Institut für Plasmaphysik, EURATOM Association,
Garching bei München, Germany

ABSTRACT

A method for obtaining efficient current drive in Tokamaks using low-phase-velocity ($v_p = \omega/k_\parallel \sim 0.1 v_{te}$) kinetic Alfvén wave is proposed.

The wave momentum, imparted primarily to the trapped electrons by Landau damping, is stored as the canonical angular momentum via the Ware pinch. In steady state, collisions restore the pinched electrons to their original phase-space configuration, in the process releasing the stored canonical angular momentum to the background ions and electrons in proportion to the respective collision frequencies. Despite the loss of a part of the original impulse to the plasma ions, well over half the wave momentum is ultimately delivered to the bulk-plasma electrons, resulting in an efficient current drive.

A normalized current-drive efficiency $\gamma = R_0 < n_{20} > I/P \sim 2$ would be feasible using the subthermal kinetic-Alfvén-wave current drive in a Tokamak of reactor parameters.

Optimum antenna loading conditions are described. The problem of accessibility is discussed. In an elongated, high-β plasma with a density dependence $n_e \sim (1-\rho^2)^{\chi_n}$, accessibility is restricted to $\rho \gtrsim 3/(4A\chi_n)$, where A is the aspect ratio. For current drive at still lower values of ρ, operation in conjunction with fast-wave current drive is suggested.

1. INTRODUCTION

In the absence of toroidal effects, the transfer of parallel momentum $\Delta v_\parallel$ to an electron produces a current $e\Delta v_\parallel$ of duration ν_{ei}^{-1} and requires an energy input $m v_p \Delta v_\parallel$, where ν_{ei} is the Spitzer collision frequency and v_p is the wave phase velocity along the static magnetic field B_0. The current density is related to the power density by

$$j = \frac{e}{m}\frac{p}{v_p \nu_{ei}} \,. \tag{1}$$

From Eq. (1), Wort [1] identified the low-phase-velocity ($v = v_p/v_{te} \ll 1$) subthermal regime as being the most suitable for current drive.

In a torus, the subthermal wave momentum is primarily imparted to the trapped electrons constituting the dominant fraction $\beta_t = \exp\left[-v^2/2\varepsilon\right]$, where $\varepsilon = \rho/A$, $\rho = r/a$, a is the plasma radius and A is the aspect ratio. Since the trapped particles do not directly contribute to the current drive, Bickerton [2] concluded that subthermal waves are unsuitable for current drive in toroidal geometry. Fisch [3] suggested that the canonical angular momentum stored by the trapped electrons via the Ware [4] pinch could cause current drive in a manner analogous to bootstrap [2] current, although a

quantitative estimate of this effect was not attempted. Confronted with the perceived complexity of momentum recovery, this hopeful stand was later reversed [5].

The strand was picked up once again by Puri and Wilhelm [6] who were able to precisely quantify the extent of recovery of the canonical angular momentum initially delivered to the trapped electrons for the purpose of current drive. Their arguments based upon the rigorous conservation of canonical angular momentum in an axisymmetric toroidal geometry are reproduced in Sec. 3.3

In another significant development, Elfimov and Puri [7] have shown that α_u, the fractional wave momentum imparted to the untrapped electrons greatly exceeds their relative abundance, $\beta_u = 1 - \beta_t$ due to the toroidal modification of Landau damping. This effect, together with the canonical angular momentum recovery, results in high current-drive efficiency for the low-phase-velocity kinetic-Alfvén-wave.

2. THE KINETIC ALFVÉN WAVE

2.1 Dispersion characteristics

Fig. 1 shows the qualitative low-frequency Alfvén wave dispersion characteristics in a slab geometry for $k_y = 0$. Plasma density and temperature are assumed to increase along x while the magnetic field is along the z direction. ϵ_x, ϵ_y and ϵ_z are the components of the dielectric tensor, $\mathbf{n} = \mathbf{k}/k_0$, and $\epsilon_{L,R} = \epsilon_x \pm \epsilon_y$. The externally launched evanescent compressional Alfvén wave (COM) partially couples to the propagating COM and is partially steered by the Hall term arising through ϵ_y to the propagating kinetic Alfvén wave (KIN) in the plasma interior. The wave converted KIN is efficiently absorbed through Landau damping giving rise to plasma heating and current drive.

In the absence of electron inertia, the KIN dispersion curve assumes the vertical stance of the well-known Alfvén resonance independently proposed by Winterberg [8] and Grossman and Tataronis [9] for plasma heating. Inclusion of electron inertia and temperature by Hasegawa and Chen [10] lead to the discovery of KIN and of Landau damping as the mechanism responsible for energy absorption.

The damping length of KIN estimated from the approximate dispersion relation

$$n_x^2 = \frac{\epsilon_z}{\epsilon_x}(\epsilon_x - n_z^2) \ , \tag{2}$$

in the absence of finite ion-gyroradius correction is given by [11]

$$[\Im k_x]^{-1} \approx \sqrt{\frac{1}{2\pi}} \frac{c}{\omega_{pe}} \frac{\exp(v^2)}{v^2} \ . \tag{3}$$

Inclusion of gyroradius correction limits $\Lambda_i = (1/2)k_x^2 r_{ci}^2$ to $\Lambda_i \lesssim 1$ so that

$$[\Im k_x]^{-1} \approx \sqrt{\frac{2}{\pi}} \frac{v_{ti}}{\omega_{ci}} \frac{\exp(v^2)}{v} \ . \tag{4}$$

In either case, the absorption length is typically only a few centimeters. For all practical purposes, KIN is absorbed close to the Alfvén resonance region $\epsilon_x = n_z^2$ even in a hot

plasma. The coupling remains materially unaffected by the finite-temperature as well as by the finite-gyroradius effects.

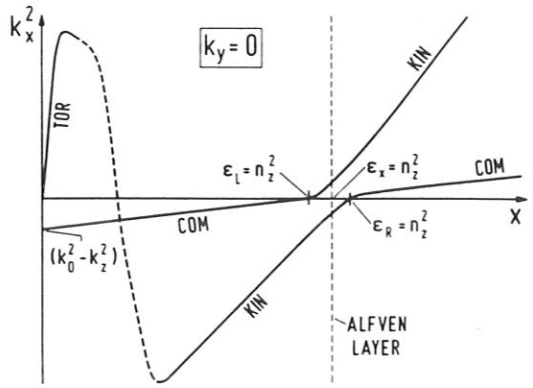

Fig. 1 Qualitative dispersion curves

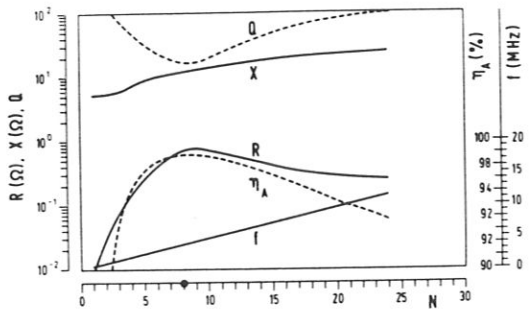

Fig. 2 Antenna loading versus N

2.2 Coupling considerations

For the $k_y = 0$ case shown in Fig. 1, coupling to propagating COM dominates over wave conversion to propagating KIN. An increase in k_y, corresponding to an upward translation of the abscissa in Fig. 1, moves the right cutoff away from the Alfvén layer and reduces coupling to the propagating COM. In cylindrical (or pseudo-toroidal) geometry this is achieved by using $m = \pm 1$ poloidal mode. Increasing k_z (or the toroidal wave number n) while maintaining the Alfvén layer fixed at a given radial location raises the frequency of operation ω; the corresponding increase in the Hall term ϵ_y is accompanied by an increased wave-conversion efficiency to KIN. Thus the combination of finite $m = \pm 1$ and large $n \sim 5 - 8$ defines the optimum coupling conditions for KIN.

The profound influence of m and n on the Alfvén wave coupling was seen in the boundary value analysis of Ross, Chen and Mahajan [12]. They included equilibrium plasma current (safety factor q) in their treatment and pointed out the enhancement of the Hall term ϵ_y by a factor

$$\left| \frac{\tilde{\epsilon}_y}{\epsilon_y} \right| \approx \frac{2}{q k_0 R_0} \frac{\omega_{ci}^2}{\omega \omega_{pi}} , \tag{5}$$

induced by the Doppler shift associated with electron drift. Another important contribution of equilibrium current is to involve m in the parallel refractive index, modifying the Alfvén resonance condition to

$$\epsilon_\xi = n_\zeta^2 = n_z^2 \cos^2 \chi \left(1 + \frac{m}{qn} \right)^2 , \tag{6}$$

where ξ, η, ζ are the *local* coordinates with the ζ axis tilted at an angle χ with respect to the z axis. In addition to heating by the wave-converted KIN, the plasma is also susceptible to undesirable surface heating by the direct excitation of torsional Alfvén wave (TOR), particularly in the twisted magnetic field geometry in the presence of the plasma current [12, 13].

Lowering ω moves the Alfvén resonance layer radially inwards to higher densities until the Alfvén resonance continuum disappears completely. Appert et al. [14]

discovered that at some still lower values of ω one encounters fluid magnetohydrodynamic resonances of the plasma column. The so-called discrete Alfvén wave resonances possess neither kinetic nor resistive absorption mechanisms [15] and are not suited for plasma heating and current drive because of the extremely high antenna $Q's$. Further references to the extensive literature on Alfvén wave heating and current drive by the Austin, Lausanne, Sydney and Sukhumi groups are to be found in Refs. [12 – 14, 16].

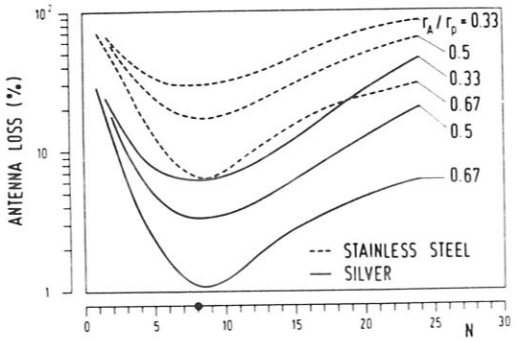

Fig. 3 Antenna losses versus N

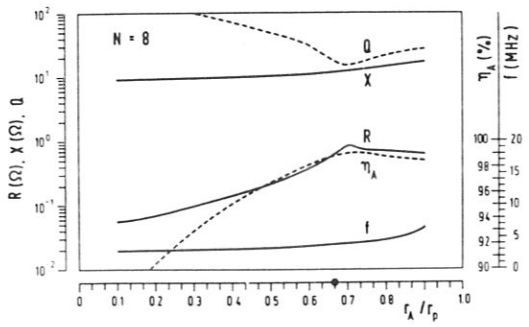

Fig. 4 Antenna loading versus ρ

2.3 Antenna configuration

Puri [17] has conducted detailed computations of antenna loading for realistic antenna configurations including feeders, finite antenna width, self-consistent current distribution, Faraday screening, kinetic effects, surface dissipation, equilibrium current and multi-mode excitation in a cylindrical plasma. Fig. 2 taken from Ref. [17] shows representative values of antenna resistance R, reactance X, quality factor Q, antenna coupling efficiency η_A (assuming silver-plated antenna) and frequency of operation f for plasma parameters corresponding to $n_0 = 3 \times 10^{20}\, m^{-3}$, $T_{e0} = 7\, keV$, $B_0 = 3T$, $q_0 \sim 1$, $q_a = 3$, and with the resonant layer located at $\rho = 0.67$ as a function of the fundamental toroidal wave number N.

It is immediately clear that low ($N < 4$) toroidal wave numbers are unsuited for coupling to KIN. As already pointed out, for low N with correspondingly low ω, the Hall term ϵ_y is too meagre to affect significant wave conversion of the launched COM to KIN. Further analytic confirmation of this assertion occurs in the Appendix of Ref. [17]; it is also shown how finite k_y ($m \neq 0$) has a salutory effect in reducing COM evanescence in conjunction with the radial gradients. The importance of using high values of N are further evident from the antenna loss curves [17] shown in Fig. 3.

However, the requirement of a finite azimuthal wave number $m = 1$ and a large toroidal wave number $n = 5 - 8$ imposes the serious penalty of limited radial access of the antenna field into the plasma due to the increased evanescence experienced by COM as shown in Fig. 4 taken from Ref. [17]. Thus, in a cylindrical geometry, it is not possible to gain access to $\rho < 2/3$ while maintaining a high antenna coupling efficiency. Fortunately, the situation improves dramatically for the practically relevant case of non-circular cross-section plasmas.

2.4 Non-circular plasma cross section and finite-β effects

In an elliptical plasma of elongation e, the antenna situated near the plasma surface in the meridian plane has a radius of curvature $r_A \approx ae^2$. The increase in r_A by the factor e^2 causes a corresponding drop in the azimuthal wave number $k_y = m/r$ while the toroidal wave number $k_z = n/R$ remains unaltered. The net effect is an enhancement in the penetration depth from $\rho = 2/3$ to $\rho = 1/3$ for $e \sim 2$ [18]. This estimate assumes that the antenna length $L_A \gtrsim a$, so that the COM evanescence is dominated by k_z, and not by the short antenna length.

Further significant enhancement in the penetration of antenna energy into the plasma interior is contributed by the finite β in a reactor-grade plasma. Finite β is accompanied by an outward shift

$$\Delta R = \psi a \ , \tag{7}$$

of the plasma axis which for the reactor parameters may amount to $0.25a$. Thus a combination of non-circular cross section and finite-β effects would ascertain efficient penetration of the antenna energy right down to the plasma core, for sufficiently peaked density profiles as discussed in the following section.

2.5 Density profile and accessibility

In Sec. 2.4 it was shown that the combination of plasma elongation and β would allow wave penetration to the plasma core through the reduction in COM evanescence. In this section yet another obstacle confronting KIN accessibility to plasma interior arising from flat density profiles is considered.

The radiofrequency power is principally deposited in the narrow vicinity of the Alfvén resonance condition

$$\epsilon_\xi \approx \frac{\omega_{pi}^2}{\omega_{ci}^2} = n_z^2 \cos^2\chi \left(1 + \frac{m}{qn}\right)^2 \ ,$$

or

$$\omega \approx k_z c \cos\chi \left(1 + \frac{m}{qn}\right) \frac{\omega_{ci}}{\omega_{pi}} \ . \tag{8}$$

In cylindrical geometry, $\omega \sim \omega_{pi}^{-1}$ decreases monotonically as the plasma center is approached. However in a torus, since $k_z\omega_{ci}$ increases as R^{-2} whereas $(1-1/qn)$ decreases roughly as R towards the plasma axis, ω goes through a minimum at

$$\rho \approx \frac{1-\psi}{A\chi_n} \ , \tag{9}$$

where ψ is the fractional outward shift of the plasma axis due to finite β. Assuming $\psi = 1/4$, accessibility till $\rho = 0.3$ requires that $A \geq 2.5/\chi_n$. For the parabolic density profile with $\chi_n = 1$, one needs $A \geq 2.5$, i.e., accessibilty is possible for all foreseeable aspect ratios. A density profile with $\chi_n = 1/2$ would demand that $A \geq 5$. Substantially flatter density profiles would require unrealistically large aspect ratios. Thus, the flattest density profile consistent with the accessibility requirements corresponds to $\chi_n \sim 1/2$.

3. CURRENT DRIVE

3.1 Current-drive efficiency

As indicated in Sec. 1, there are two distinct contributions to current drive. A fraction α_u of the wave momentum (power) is directly given to the untrapped electrons. These drive a current

$$j_u = \frac{e}{m}\frac{\alpha_u p}{v_A \tilde{\nu}_{ei}} , \tag{10}$$

where $v_A = c/n_z$ is the Alfvén speed and $\tilde{\nu}_{ei} = \nu_{ei}/(1-\sqrt{\varepsilon})$ is the Spitzer collision frequency enhanced by the trapped particle effects [19]. The method for determining α_u, given in Ref. [7], is briefly reviewed in Sec. 3.2. The remaining fraction $\alpha_t = 1-\alpha_u$ of the wave momentum is stored as canonical angular momentum in the trapped-electron population via the Ware [4] pinch. Under steady-state conditions, collisions transfer a fraction σ of this stored canonical angular momentum to the bulk-plasma electrons. The corresponding current is given by

$$j_t = \frac{e}{m}\frac{\sigma\xi\alpha_t p}{v_A \tilde{\nu}_{ei}} , \tag{11}$$

where $\xi = 1-\sqrt{\varepsilon}$ is the fraction of the bulk-plasma electrons partaking in current drive. The momentum-recovery index σ was determined in Ref. 6; the relevant arguments are outlined in Sec. 3.3. The total current $j = j_u + j_t$ induced by p becomes

$$j = \frac{e}{m}\frac{\alpha_u + \sigma\xi\alpha_t}{v_A\tilde{\nu}_{ei}} p = \frac{p}{\Gamma} , \tag{12}$$

where

$$\Gamma = \frac{m}{e}\frac{v_A\tilde{\nu}_{ei}}{\alpha_u + \sigma\xi\alpha_t} . \tag{13}$$

Equation (12) prescribes the power density profile $p(\rho) = \Gamma(\rho)j(\rho)$ required to impose a specified current density profile $j(\rho)$. The normalized current-drive efficiency becomes

$$\gamma = < n_{20} > R_0 \frac{I}{P} = \frac{< n_{20} >}{2\pi}\frac{\int_0^1 j(\rho)\rho\, d\rho}{\int_0^1 \Gamma(\rho)j(\rho)\rho\, d\rho} , \tag{14}$$

where R_0 is the torus major radius, $I = \int j\, dS$, $P = \int p\, dV$, and $< n_{20} > \times 10^{20}\, m^{-3}$ is the volume-averaged plasma density.

The current-density profile is dependent upon q_a, the safety factor at the plasma edge and upon the available bootstrap current I_b. Maximum current-drive efficiency is obtained if the wave-driven seed current $I_s = I_p - I_b$ is spread with a constant density j_s in the region $0 \le \rho \le \rho_s \approx \sqrt{I_s/q_a I_p}$, where $j_s = (2/R_0)(B_t/\mu_0)$ is the maximum current density consistent with the MHD stability requirement $q_a \ge 1$. Equation (14) assumes the simple form

$$\gamma_s = \frac{< n_{20} >}{2\pi}\frac{\int_0^{\rho_s} \rho\, d\rho}{\int_0^{\rho_s} \Gamma(\rho)\rho\, d\rho} . \tag{15}$$

An alternate useful figure of merit is contained in the effective current-drive efficiency given by

$$\gamma_{eff} = (I_p/I_s)\,\gamma_s \ . \tag{16}$$

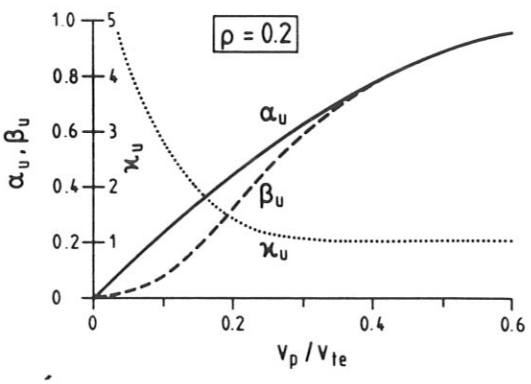

Fig. 5 α_u and β_u versus υ

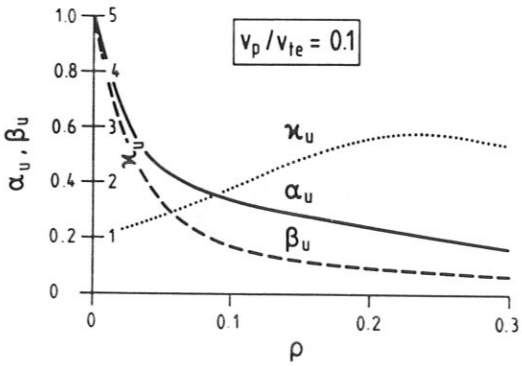

Fig. 6 α_u, β_u and κ_u versus ρ

3.2 Toroidal modification of Landau damping

The extreme variation in $v_{\|}$ encountered by the particles in toroidal geometry, most particularly by the trapped particles, is accompanied by modification in Landau damping. Using the theory developed by Grishanov and Nekrasov [20], it is found [7] that α_u, the fraction of the wave momentum imparted to the untrapped electrons considerably exceeds their relative abundance β_u. Figs. 5 and 6 taken from Ref. 7 show α_u, β_u and $\kappa_u = \alpha_u/\beta_u$ as functions of υ and ρ, respectively, for representative Tokamak reactor parameters. For $\upsilon \sim 0.1$ for the case of KIN current drive, $\alpha_u \sim 0.25$ while $\beta_u \sim 0.1$. The weakened Landau damping causes the KIN absorption length to increase beyond the value given in Eq. (4), thereby adding to the energy penetration depth into the plasma core.

3.3 Canonical-angular-momentum recovery

Despite the appreciable momentum transfer to the circulating electrons, the bulk $\alpha_t = 1 - \alpha_u \sim 0.75$ of the wave momentum goes into the trapped electrons which do not directly contribute to current drive. Conservation of canonical angular momentum for a trapped electron in a radio-frequency-driven steady-state Tokamak implies [21]

$$\frac{d}{dt}\left[mRv_\varphi + \frac{eRE_\varphi}{\omega - k_\varphi v_\varphi}\cos\{(\omega - k_\varphi v_\varphi)t\} + \frac{e}{2\pi}\Phi\right] = 0 \ , \tag{17}$$

where the last two terms in the square brackets are contributed by eRA_φ, A_φ is the vector potential, $(R,\ \varphi,\ z)$ are the cylindrical coordinates, $\Phi = \int_0^R 2\pi RB_z\,dR$, and B_z is the z component of the magnetic field due to the plasma current. Under resonant interaction of duration Δt, the electron gains (assuming favorable phase relative to the electric field) an angular momentum

$$R\Delta p_\varphi = mR\Delta v_\varphi = eRE_\varphi\Delta t = \frac{e}{2\pi}(\Phi_0 - \Phi) = \frac{e}{2\pi}\,\Delta\Phi \ , \tag{18}$$

and is pinched inwards from flux surface Φ_0 to Φ (Fig. 7). In steady state, collisions restore the particle to its original orbit with its starting velocity $v_{\varphi 0}$ and the flux surface Φ_0, in the process releasing a mechanical momentum Δp_φ to the background ions and electrons *in proportion* to their respective collision frequencies. Thus the wave acts as a continuous pump delivering angular momentum to the trapped electrons resonant with the wave; whereas collisions redistribute the momentum to the bulk plasma over a period lasting $\varepsilon(\nu_{ee} + \nu_{ei})^{-1}$. Alternatively, the collisions may be modeled by an appropriate electric-field-spectrum term in Eq. (17). Summing Eq. (17) over the ensemble of accelerated population and requiring $\sum \Delta p_\varphi = 0$ (since $\sum \Delta v_{\varphi 0} \equiv 0$ and $\sum \Delta \Phi \equiv 0$ in the steady state) shows that the mechanical momentum imparted by the pump wave to the accelerated particle population is redistributed to the background plasma in the manner already described. The fraction of the recovered canonical angular momentum transferred to the bulk-plasma electrons is given by

$$\sigma = (1 + \nu_{ei}/\nu_{ee})^{-1} \approx (1 + 0.5Z)^{-1} \ . \tag{19}$$

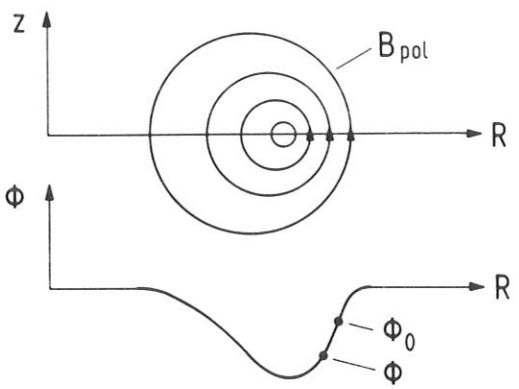

Fig. 7 Tokamak flux surfaces

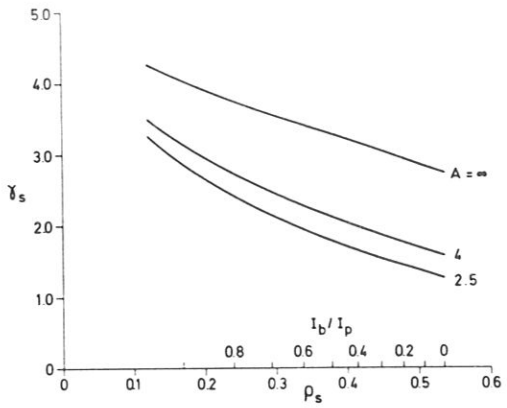

Fig. 8 Current-drive efficiency

3.4 Computational results

Assuming $n_e(\rho) = n_{e0}(1-\rho^2)^{\chi_n}$ and $T_e(\rho) = T_{e0}(1-\rho^2)^{\chi_T}$ in Eq. (15), one obtains

$$\gamma_s = \frac{13.5\mu^{1/2} < \beta >^{1/2} < T_{keV} > \int_0^{\rho_s} \rho \, d\rho}{Z < \ln\Lambda > \int_0^{\rho_s} (\alpha_u + \sigma\xi\alpha_t)^{-1}(1-\rho^2)^{-\chi}\xi^{-1}\rho \, d\rho} \frac{\chi_T + 1}{\chi_n + 1}(\chi_T + \chi_n + 1)^{1/2} \ , \tag{20}$$

where μ is the atomic mass number, $< \beta >$ is the volume-averaged toroidal β, $< T_{keV} >$ is the volume-averaged electron temperature in keV, $< \ln\Lambda >$ is the weighted Coulomb logarithm, and $\chi = 1.5\chi_T - 0.5\chi_n$. Fig. 8 is a plot of γ_s as a function of $\rho_s = \sqrt{I_s/q_a I_p}$ and A for $\chi_n = 1$, $\chi_T = 1.5$, $\mu = 2.5$, $< \beta >= 0.05$, $< T_{keV} >= 15$, $Z = 1.5$, $q_a = 3.5$, $\ln\Lambda = 17$ while Figs. 5 and 6 are used to approximate α_u as

$$\alpha_u(v, \rho) = (11v - 16v^2 + 20v^3)\exp(-9\rho + 11\rho^2) \ . \tag{21}$$

Fig. 8 shows that for $0.1 \leq I_b/I_p \leq 0.9$, one obtains a seed-current-drive efficiency in the range $1.5 \leq \gamma_s \leq 3$ which is at least five times higher than the corresponding

figures for alternative non-inductive current-drive schemes. In fact, reactor-relevant operation with $\gamma_s \sim 1.5$ is possible without any reliance on the bootstrap current.

3.5 Effect of Matsuda anomaly on momentum recovery

Matsuda anomaly predicts an enhancement of electron-ion momentum-transfer collisions parallel to the magnetic-field direction for electrons with $r_{ce} < \lambda_D$ and $v_{\|e} \sim v_{ti}$, where λ_D is the Debye length [22,23]. If ν_{ei} were to be significantly augmented above its Spitzer value, the proportion of the canonical angular momentum received by the bulk-plasma ions would increase, while that given to the bulk-plasma electrons would decrease. Consequently, the current-drive efficiency would be diminished.

Fortunately, however, since the increased collisionality is exhibited precisely where the colliding electrons possess little parallel momentum, the net effective increase in ν_{ei} is negligible. In Ref. [24] it is shown that in the hot plasma interior where current drive is intended, the Matsuda anomaly contributes almost no loss of canonical angular momentum from the trapped electrons to the ions. This is despite the fact that the ion-velocity-distribution model employed in Ref. [24] tends to overestimate the Matsuda anomaly contribution.

Hence one may use the ratio of Spitzer collision frequencies with confidence in allocating the relative proportions of the recovered canonical angular momentum to the bulk-plasma ions and electrons.

4. DISCUSSION AND CONCLUSIONS

Of the two possible wave-driven non-inductive current-drive schemes, the one using fast waves is by far the most popular. In the recently held international radiofrequency application conference [25] the slow-wave current drive is not even represented. This is the result of legitimate apprehensions regarding (i) the role of trapped electrons on current drive, and (ii) the feasibility of efficient coupling of the evanescent low-frequency COM and its subsequent conversion to KIN in an efficient manner.

The present paper reviews, corrects and enlarges on the existing knowledge on the subject. The objection concerning the calamitous role of trapped particles is found to be faulty on two counts, namely (a) the markedly stronger tendency of the circulating electrons to absorb wave momentum via Landau damping [7] in comparison with their trapped counterparts leads to a significantly stronger current drive than that expected from their relative abundance, and (b) the momentum absorbed by the trapped particles is not to be disregarded; it reappears through collisions to drive significant current.

Efficient coupling ($\eta_A \sim 1$), at moderate $Q \sim 14$ and antenna voltage $V \sim 14\,kV$ for $1\,MW$ input, is possible using ~ 20 antenna sections phased $\pi/2$ apart. The problem of wave accessibility is more serious. Although the problem of COM evanescence in high-β plasmas can be solved by using elongated cross sections, one is still confronted with accessibility restrictions caused by flat density profiles in combination with low aspect ratios. Assuming that the maximum acceptable $A = 5$, gives the flattest density profile corresponding to $\chi_n = 1/2$. If current drive for $\rho \leq 0.3$ is deemed necessary, one would need to use KIN current drive (for $0.3 \leq \rho \leq 0.6$) in conjunction with fast-wave current drive (for $\rho \leq 0.3$).

The most heartening and significant feature is that it is possible to obtain reactor-relevant performance using KIN current drive—a doubtful prospect with any of the currently available alternatives [26]—in the region $0.3 \leq \rho \leq 0.6$, provided that $\chi_n \geq 0.5$. The seed current-drive efficiency figures are approximately five times higher than other non-inductive approaches. A serious and concerted effort to further develop the KIN current-drive scheme is warranted.

ACKNOWLEDGMENTS

I am thankful to Prof. R. Wilhelm and Dr. A. Elfimov for being able to use the information contained in Refs. [6], [7] and [18].

REFERENCES

[1] WORT, D.J.H., Plasma Phys. **13** (1971) 258.
[2] BICKERTON, R.J., Comments Plasma Phys. Controll. Fusion **1** (1972) 95.
[3] FISCH, N.J., in Proceedings of Second Joint Varenna-Grenoble International Symposium on Heating in Toroidal Plasmas, Como, 1980, CEC, Brussels (1980) 1157.
[4] WARE, A.A., Phys. Rev. Lett. **25** (1970) 15.
[5] FISCH, N.J., Rev. Mod. Phys. **59** (1987) 175.
[6] PURI, S., WILHELM, R., in Radio-Frequency Power in Plasmas (Proc. 8th Top. Conf., Irvine, CA, 1989) Conf. Proc. No. 190, APS, New York (1989) 458.
[7] ELFIMOV, A.G., PURI, S., Nucl. Fusion **30** (1990) 1215.
[8] WINTERBERG, F., Ann. Phys. **25** (1963) 174.
[9] GROSSMAN, W., TATARONIS, J.A., Z. Phys. **261** (1973) 217.
[10] HASEGAWA, A., CHEN, L., Phys. Rev. Lett. **32** (1974) 454.
[11] PURI, S., in Plasma Physics and Controlled Nuclear Fusion Research 1980 (Proc. 8th Int. Conf. Brussels, 1980), Vol.2, IAEA, Vienna (1981) 51.
[12] ROSS, D.W., CHEN, G.L., MAHAJAN, S.M., Phys. Fluids **25** (1982) 652.
[13] BALLICO, M.J., et al. Plasma Phys. Controll. Fusion **30** (1988) 1331.
[14] APPERT, K., et al. Nucl. Fusion **22** (1982) 903.
[15] BERNSTEIN, I., Phys. Fluids **26** (1983) 730.
[16] SIDOROV, V.P., et al Nucl. Fusion **27** (1987) 1411.
[17] PURI, S., Nucl. Fusion **27** (1987) 1091.
[18] PURI, S., WILHELM, R., in Proc. 16th EPS, Venice (1989) 1315.
[19] WESSON, J., in Tokamaks, Clarendon Press, Oxford (1987) 95.
[20] GRISHANOV, N.I., NEKRASOV, F.M., Fiz. Plasmy **16** (1990) 230.
[21] PANOFSKY, W.K.H., PHILLIPS, M., in Classical Electricity and Magnetism, Addison-Wesley, London (1962) 431.
[22] MATSUDA, K., Phys. Rev. Lett. **49** (1982) 1486.
[23] WARE, A.A., Phys. Rev. Lett. **62** (1989) 51.
[24] PURI, S., in Proc. 18th EPS, Berlin, (1991) IV-209.
[25] Ninth Top. Conf. on RF Power in Plasmas, Charleston, SC (1991).
[26] KNOBLOCH, A.F., Steady-State Operation Requirements of Tokamak Fusion Reactor Concepts, Max-Planck-Institut für Plasmaphysik Report IPP 4/246 (1991).